IEEE Access
Multidisciplinary | Rapid Review | Open Access Journal

SPECIAL SECTION ON TOWARDS SMART CITIES WITH IOT BASED ON CROWDSENSING

Received December 15, 2020, accepted January 6, 2021, date of publication January 13, 2021, date of current version January 25, 2021.

Digital Object Identifier 10.1109/ACCESS.2021.3051389

AoA-Based Localization System Using a Single IoT Gateway: *An Application for Smart Pedestrian Crossing*

NOORI BNILAM[1], (Member, IEEE), DENNIS JOOSENS[1], RAFAEL BERKVENS[1], (Member, IEEE), JAN STECKEL[2,3], (Member, IEEE), AND MAARTEN WEYN[1], (Member, IEEE)

[1]IDLab, Faculty of Applied Engineering, imec, University of Antwerp, 2000 Antwerp, Belgium
[2]Cosys-lab Research Group, University of Antwerp, 2000 Antwerp, Belgium
[3]Flanders Make Strategic Research Center, 3920 Lommel, Belgium

Corresponding author: Noori Bnilam (noori.bnilam@uantwerpen.be)

This work was supported by the Flemish Agency for Innovation and Entrepreneurship (VLAIO) through funding the Observer Project.

ABSTRACT During the last decade, the concept of smart cities is gaining popularity, and many cities all around the globe are adopting it. Lately, the Smart Pedestrian Crossing (SPC) idea has become an important part of the smart city concept. The main objective of the SPC is to achieve a safe and smooth traffic flow of pedestrians and vehicles in the smart city. In this paper, we present a simple yet efficient localization system which is suitable for locating people over a pedestrian crossing. By adopting the proposed localization system, the people flow over the pedestrian crossing can be observed. Consequently, a safe and efficient traffic flow in the smart city can be achieved. The proposed system utilizes Internet of Things (IoT) transceivers that are carried by the pedestrians or embedded in the pedestrians' smart devices. These transceivers can be activated to transmit a signal every few seconds when the pedestrian passes over a pedestrian crossing. These periodic signals will be received by a single Angle of Arrival (AoA) estimation system to estimate the direction of the pedestrian. Furthermore, the pedestrian direction and the environmental features of the pedestrian crossings are utilized in a 1D particle filter to estimate accurately the pedestrian's location. The proposed system has been validated experimentally in the smart zone of Antwerp city. The experimental results reveal that the proposed localization system can provide an accurate, cost effective and reliable localization solution to this specific problem without violating the pedestrian privacy.

INDEX TERMS AoA, angle of arrival, DoA, direction of arrival, Internet of Things, IoT, environmental features localization, smart pedestrian crossing, smart cities, particle filter, SAGE algorithm.

I. INTRODUCTION

Henceforth the 1990s, digital communication systems have been under enormous developments. Most of these developments are concerned with increasing the throughput, decreasing the latency and improving the quality of service of the communication systems. Nowadays, the industry demands have been shifted towards the smart systems idea. These demands are the key factor to the birth of the Internet of Things (IoT) technology. Consequently, low power wireless area network (LPWAN) standards (such as LoRa [1], Sigfox [2] and NB-IoT [3]) and low power communication standards (such as DASH7 [4]) are currently providing IoT services. This communication revolution can be attributed to few reasons such as: i) the reduction of the IoT transceivers' cost and size, ii) the capability of the IoT transceivers to establish long range communication links (covering area of several kilometers), and iii) the low energy consumption of the IoT transceivers. Therefore, a small and affordable IoT transceiver is expected to operate for years using a small battery.

Shortly after the introduction of the IoT technology, the concept of smart cities started to verbalize [5]. Hence, many cities all over the globe have started to deploy this concept. For instance, in the city of Antwerp in Belgium, a part of the city has been dedicated to be a smart zone [6], companies and research institutes are encouraged to deploy any connectivity technology in a real life environment. Lately, the idea of the Smart Pedestrian Crossing (SPC) has been introduced as an important part of the smart city concept [7].

The associate editor coordinating the review of this manuscript and approving it for publication was Zhibo Wang.

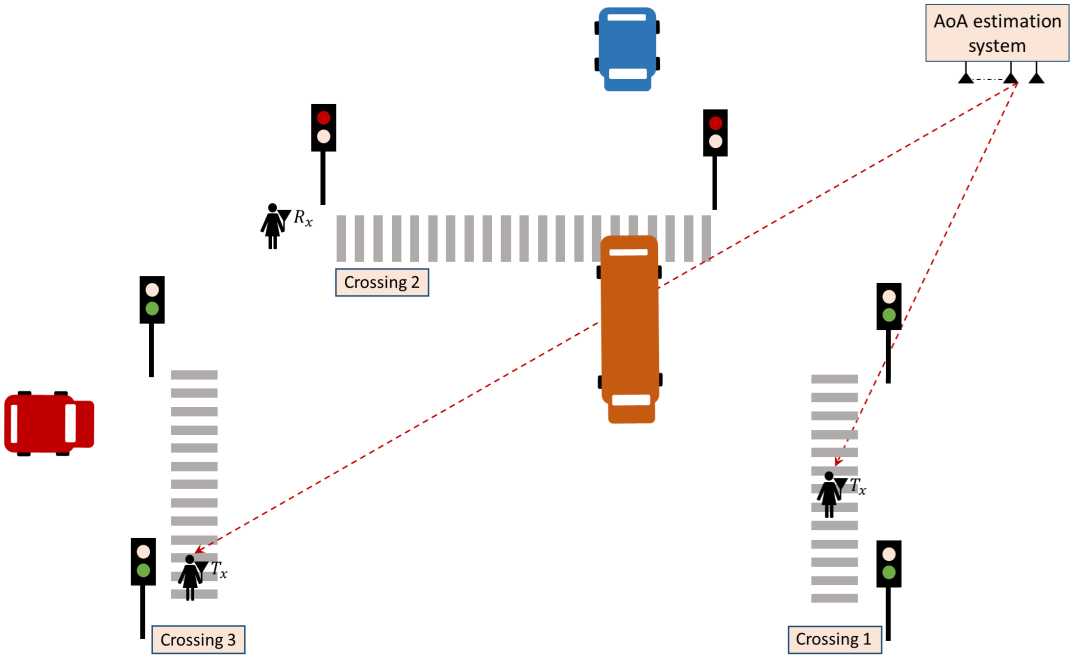

FIGURE 1. A schematic representation of the proposed localization system. The figure shows that the proposed system can, simultaneously, monitor several pedestrian crossings. Consequently, some crossings might be situated at the same direction with respect to the AoA estimation system. In this case, an ambiguity in locating the pedestrian might occur (e.g. identification ambiguity between crossing 2 and 3). Therefore, we deployed a particle filter that exploits the previous measurements to resolve this ambiguity. Furthermore, due to the deployment of the particle filter, the proposed localization solution is less influenced by the presence of instantaneous obstacles (e.g. the big bus between crossing 3 and the AoA system) compared with camera-based solutions.

The deployment of the SPC should provide a safe passage to people over the pedestrian crossing, and a smooth traffic flow to vehicles in the smart city. Many solutions were proposed to tackle these challenges. Some solutions were concerned with controlling the pedestrians and vehicles flow in streets' intersections [8] and [9]. Other solutions were concerned with the safety of the people over a pedestrian crossing [10]. Apparently, to the best of the authors' knowledge, no solution has been introduced yet to tackle the both challenges of the SPC. Therefore, tackling these challenges in a single solution constitutes the main objective of this paper.

Achieving a safe and smooth flow of people and vehicles over a pedestrian crossing is a challenging task. Depending on the age and the health, people speeds vary as they walk over a pedestrian crossing. Therefore, in many occasions, the traffic lights turn green for the cars while people are still walking over the pedestrian crossing. In these occasions, the traffic flow will be disturbed, and the people safety will be jeopardized. Thus, on such an occasion, the traffic can be handled ''smartly'', by keeping the traffic lights red for the cars to allow a safe passage for the pedestrian, meanwhile other traffic lights (where the pedestrian crossing is idle) can keep the green lights for a longer period. Thus, by adopting this approach, a safe and efficient traffic flow in the city can be achieved.

Observing the pedestrian location on the pedestrian crossing can provide a safe passage for the pedestrians and an optimized traffic flow for the vehicles. Solutions based on cameras [11] and radars [12] can be adopted to monitor the pedestrian crossing. In general, camera-based solutions are not preferred due to privacy issues and the dependency of cameras on a clear visual sight of the pedestrian crossing which is not always guaranteed. Radar-based solutions, on the other hand, are less influenced by the environmental and weather changes than cameras. Nevertheless, the installation of radar monitoring system for every pedestrian crossing is a high cost ánd maintenance solution.

In this paper, we proposed a new low cost and efficient localization solution that can estimate the pedestrian location on the pedestrian crossing. The proposed system utilizes IoT transceivers carried by the pedestrians or embedded in the pedestrians' smart devices[1]. These transceivers can be activated to transmit every few seconds when the user passes over a pedestrian crossing. These periodic signals will be received by a single Angle of Arrival (AoA) estimation system to estimate the direction of the pedestrian. Furthermore, the pedestrian direction and the environmental features of the pedestrian crossings are utilized in a 1D particle filter to estimate accurately the pedestrian location.

Figure 1 shows a schematic representation of the proposed localization system. The figure reveals that the proposed

[1] It is worth noting that the upcoming 5G technology will enable the massive Machine Type Communications (mMTC). The mMTC component will complement the machine-type communications technologies known as LTE-M and Narrow Band IoT (NB-IoT), which are already developed by 3GPP in Rel-13 [13]. Therefore, IoT transceivers are expected to be massively deployed for various applications in the near future.

system can, simultaneously, monitor several pedestrian crossings. Consequently, as shown in the figure, some crossings might be situated at the same direction with respect to the AoA estimation system. In this case, an ambiguity in locating the pedestrian might occur (e.g. identification ambiguity between crossing 2 and 3). Therefore, we deployed a particle filter that exploits the previous measurements to resolve this ambiguity. Furthermore, due to the deployment of the particle filter, the proposed localization solution is less influenced by the presence of instantaneous obstacles (e.g. the big bus between crossing 3 and the AoA estimation system) compared with camera-based solutions. The contribution of this paper can be summarized as follows:

1) We introduce an unprecedented localization solution based on IoT technology to tackle the SPC challenges.
2) The proposed localization system can monitor several crossings simultaneously, making it a compact and cost effective localization system. Radar-based solution, on the other hand, requires the installation of radar monitoring system for every pedestrian crossing.
3) The proposed localization system, compared to a camera-based solution, is independent of the environmental and weather changes.
4) The proposed system utilizes, innovatively, few components to provide a novel localization system. The proposed system constitutes low cost IoT transceivers, a low cost array antenna system, an efficient AoA estimation algorithm, and a particle filter implementation.

The remainder of this paper is structured as follows: In Section II, the localization approach of the proposed system is introduced. Section III presents an overview of the proposed system's components. The experimental setup and results are discussed in Sections IV. Finally, the conclusions are drawn in Section V.

II. THE LOCALIZATION APPROACH

Over the past decades, several techniques have been developed and deployed to provide localization solutions. These techniques depend on either the Received Signal Strength (RSS), the Time of Arrival (ToA), the Time Difference of Arrival (TDoA) or the Angle of Arrival (AoA) parameters of the received signals [14]. RSS and time-based approaches estimate the distance between the transmitter and the receiver by measuring the signal strength and the travel time of the received signal, respectively. AoA-based approaches, on the other hand, estimate the angle between the transmitter and the receiver by measuring the phase of the received signal at different points in space using array antennas.

Localization and tracking services are considered a key feature that distinguishes IoT standards from each other. For instance, LoRa networks provide a localization solution based on the TDoA of the received signals [15]. Sigfox and NB-IoT networks, on the other hand, provide localization solutions based on the RSS values [16]. Even though the AoA estimation techniques have the potential to provide an accurate localization solution for IoT applications [17], commercially available AoA-based localization systems (to the best of the authors' knowledge) do not yet exist for IoT applications.

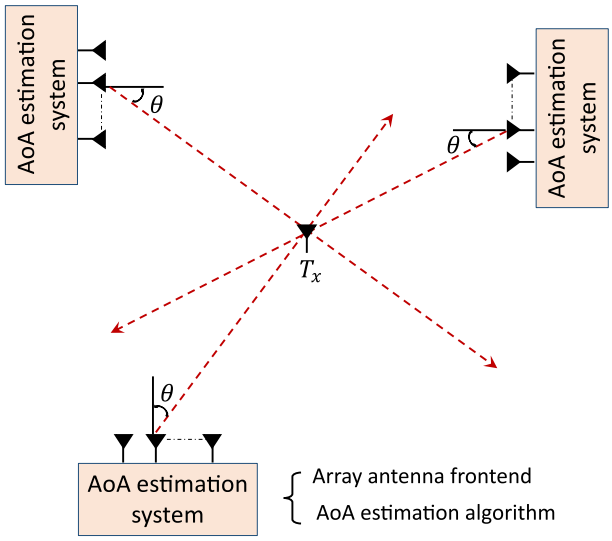

FIGURE 2. A schematic representation of an AoA-based localization system. The figure shows that AoA-based localization requires multiple spatially distributed AoA estimation systems. Every AoA estimation system constitutes an array antenna frontend and an AoA estimation algorithm. These AoA estimation systems can provide the relative directions of the received signal. Combining the direction information from every array antenna can provide a location estimate of the transmitting device.

AoA-based localization require multiple spatially distributed AoA estimation systems to provide a location estimate of the transmitting device. As shown in Figure 2, every AoA estimation system constitutes an array antenna frontend and an AoA estimation algorithm. These AoA estimation systems can provide the relative directions of the received signal. Combining the direction information can provide a location estimate of the transmitting device. Accordingly, AoA-based localization solutions based on multiple AoA estimation systems have been discussed, thoroughly, in the literature [14], [17]–[21]. For instance, Tomic *et al.* [21] provided a solution to localize outpatients in a hospital. The outpatient position can be determined by a smartphone through a geometric calculation based on the AoA estimates from two known WiFi access points.

In this paper, however, we propose a localization solution that can estimate the transceiver location based on a single AoA estimation system and the utilization of the environmental features. The proposed localization solution is suitable for locating a pedestrian over a pedestrian crossing. Figure 3 shows a schematic representation of the proposed system. The figure demonstrates that the traffic light is equipped with an IoT transmitter. This transmitter is used as a trigger to enable the pedestrian transceiver when the pedestrian traffic light changes to green. Figure 3 a) shows that the pedestrian transceiver, during the waiting period, is at the receiving mode and waiting for the trigger signal from the traffic light transmitter. Figure 3 b) implies that the pedestrian transceiver,

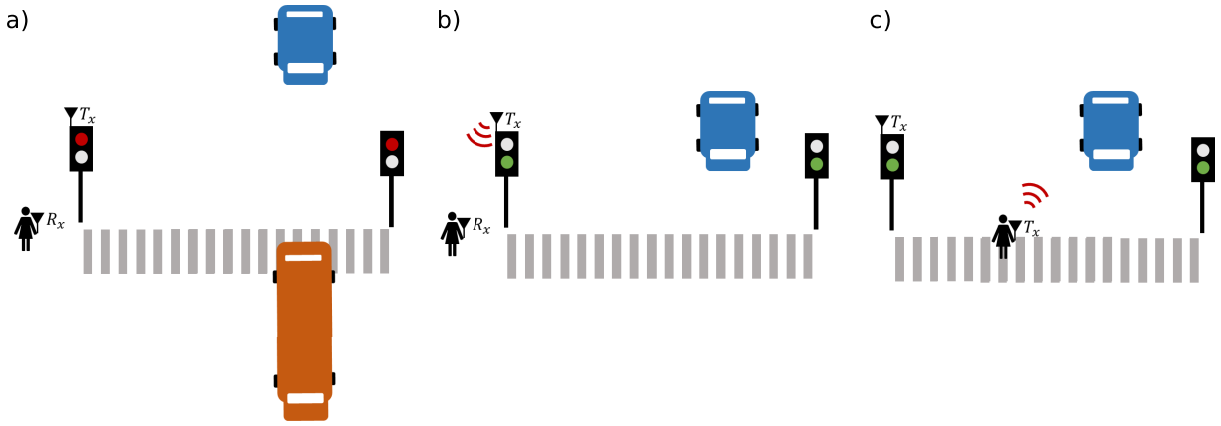

FIGURE 3. A schematic representation of the proposed system. The figure demonstrates that the traffic light is equipped with an IoT transmitter. Figure a) shows that the pedestrian transceiver is at the receiving mode. Figure b) implies that the pedestrian transceiver, as soon as the traffic light becomes green, will receive an enabling signal to change its function from a receiver to a transmitter. Figure c) shows that the pedestrian transceiver transmits periodic signals to the AoA system for the localization purpose.

as soon as the traffic light becomes green, will receive an enabling signal to change its function from a receiver to a transmitter. Figure 3 c) shows that the pedestrian transceiver, during the pedestrian walk over the crossing, transmits periodic signals to the AoA system for the localization purpose. Finally, when the pedestrian passes the crossing safely, it will get a trigger signal from the AoA system (not shown in the figure) to disable the transceiver transmission.

III. THE PROPOSED SYSTEM COMPONENTS

The proposed system consists of two main modes: the waiting and the localization modes. As shown in Figure 3, the IoT transceiver stays at the waiting mode until it receives an enabling signal from the traffic light. Afterwards, the system switches to the localization mode (i.e. the IoT transceiver starts transmitting periodic signals to the AoA estimation system for the localization purpose). The main focus of this paper is to investigate the localization capability of the proposed system. Therefore, the waiting mode has neither been implemented nor investigated. The investigation of the waiting mode will constitute the focus of the future work.

The localization mode of the proposed system consists of few components. These components are divided into hardware and software components. The hardware components include the IoT transceiver and the array antenna frontend. The software components, on the other hand, include the AoA estimation algorithm and the particle filter implementation. These components are presented hereafter:

A. IoT TRANSCEIVER

In this work, we deployed a USB transceiver (see Figure 4) based on EZR32LG Wireless Micro Controller Unit (MCU) [22]. The transceiver transmits DASH7 packets. The DASH7 is an open source standard for wireless communication over unlicensed Sub-1 GHz bands specified and promoted by the DASH7 Alliance [23]. The DASH7 standard is considered a low power mid-rang communication

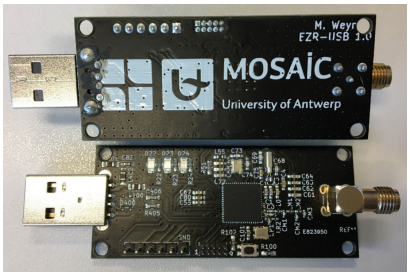

FIGURE 4. The USB transceiver that was utilized in the experiment.

standard. It can establish a communication link within sub-1 km distance, making it a suitable candidate for the problem in hand. DASH7 RF signals are formed by applying a Gaussian Frequency Shift Keying (GFSK) modulation scheme. In our experiment, the USB transceiver transmits a Lo−Rate DASH7 signal at Ch0 (i.e center frequency equals to 863MHz).

It is worth noting that BniLam *et al.* [17] had provided an energy consumption budget for the utilized transceiver. According to their analysis, the current consumption over time is approximately 0.18 μAh. Since the voltage is 3.3 V, the power consumption over time is approximately 0.6 μWh. This leads to an energy consumption per transmission of 2.2 mJ. Therefore, assuming a coincell cr2032 battery with 2268 J capacity, it is possible to have around million transmissions. Accordingly, by assuming 10 transmissions per crossing and 10 crossings per day, the user should expect to change the coincell battery after 25 years of operation.

B. ARRAY ANTENNA FRONTEND

As stated previously, any AoA estimation system requires the deployment of an array antenna at the receiver side. Several array antenna systems, that can provide AoA estimations for IoT applications, have been proposed lately [24]–[28]. These array antennas utilize either hardware or software solutions

to reduce the cost and the complexity of the array antenna system.

Recently, we introduced the RTL-Array as an AoA estimation unit for IoT applications [29]. The RTL-Array is a low cost hardware solution based on converting multiple individual low cost software defined radios (called RTL-SDR [30]) into a single SDR with multiple coherent RF-channels[2] (i.e. the RF-channels are synchronized in time and frequency, and coherent in phase). The RTL-Array unit captures the received signals in an Inphase and Quadrature (I/Q) complex data format. The I/Q data can be utilized for estimating the AoA of the received signals. The angular estimation accuracy of the RTL-Array was verified in an anechoic chamber. The estimated AoA accuracy (for a Uniform Linear Array ULA consists of 6 antenna elements) was below 1 degree in the 868 MHz frequency band. However, the RTL-Array has a limited receiving bandwidth; it can only provide a maximum receiving bandwidth of around 2.5 MHz. Nevertheless, for IoT applications, this bandwidth limitation will suffice.

In this work, a single RTL-Array has been deployed to estimate the AoA of the received signals in an outdoor environment. The RTL-Array was connected to an ULA antenna consists of 6 half wave length dipoles with inter-element spacing equals a half wavelength, as shown in Figure 5. The operating frequency was 863 MHz and the sampling rate was 1 M samples per second.

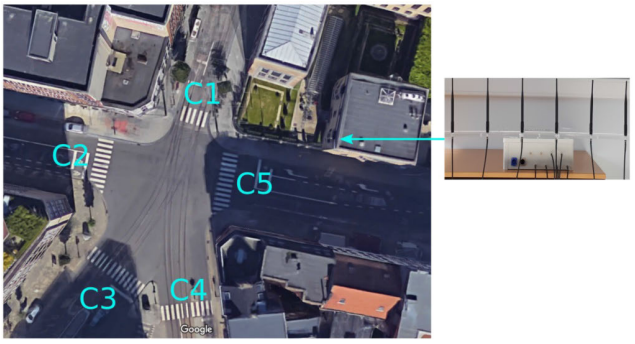

FIGURE 5. The experimental setup. The AoA unit was installed on the top of a building that faces an intersection of 5 streets. Every street has its own pedestrian crossing.

In order to present the data model of the received signals, lets assume a narrowband signal (in the far field region) that reaches an array antenna system. The array antenna is assumed to be constructed of N antenna elements. Then, the received sampled signal vector at the time index k can be expressed as

$$x(k) = [x_1(k) \dots x_n(k) \dots x_N(k)]^T , \tag{1}$$

in which

$$x_n(k) = r(k - \tau)e^{i2\pi \Delta f k} e^{i\psi_n} + \omega_n(k), \tag{2}$$

[2] For further information regarding the hardware architecture, the reader is referred to [31].

where $()^T$ is the transpose notation, τ is the propagation time delay of the received sample $r(k)$, Δf is the frequency offset between the transmitter and the receiver, and $\omega_n(k)$ is the identically independently distributed (iid) complex-valued Gaussian noise with zero-mean and variance σ^2, i.e. $CN(0, \sigma^2)$.

The time and frequency synchronization is out of this paper scope. Therefore, in the following, we will consider the simplified version of (2), as follows

$$x_n(k) = r(k)e^{i\psi_n} + \omega_n(k), \tag{3}$$

ψ_n is the phase difference between the n^{th} antenna element in the array antenna and a reference point in space. ψ_n is a function of θ and ϕ, where $\{\theta \in \mathbb{R} : -\pi \leq \theta \leq \pi\}$ is the azimuth angle and $\{\phi \in \mathbb{R} : 0 \leq \phi \leq \pi\}$ is the elevation angle. In this paper, however, we adopted the uniform linear array (ULA) antenna system, therefore, the phase response is expressed in terms of θ only, as follows

$$\psi_n(\theta) = \frac{2\pi}{\lambda} d_n \sin(\theta) , \tag{4}$$

where λ is the operational wavelength and d_n is the displacement of the n-th antenna element with respect to a specific point in space.

C. AoA ESTIMATION ALGORITHM

Over the years, several AoA estimation algorithms have been proposed [14]. In general, there are four main kinds of algorithms; algorithms that are based on an optimal beamforming, algorithms that rely on signal and noise subspaces' decomposition, algorithms that employ the parametric search using maximum likelihood (ML) estimator, and algorithms that apply the sparse representation of the space.

Here, we adopted the space alternating generalized expectation-maximization (SAGE) algorithm [32]. The SAGE algorithm employs the ML estimator to estimate the received signals parameters. The SAGE algorithm can estimate the AoA of correlated signals efficiently based on few received signals' samples, making it perfect for estimating the direct and the reflected paths of the received signal. In this paper, we adopted the implementation of the SAGE algorithm as presented by Chung and Bohme (2002) [33].

Assume there are M narrowband signals were generated in the far-field region, then, the received signal vector can be expressed as follows

$$x(k) = \mathbf{D}\mathbf{r}(k) + \mathbf{\Omega}(k), \tag{5}$$

where $\mathbf{D} \in \mathbb{C}^{N\times M}$, $\mathbf{r}(k) \in \mathbb{C}^{M\times 1}$ and $\mathbf{\Omega}(k) \in \mathbb{C}^{N\times 1}$ are the steering matrix, the received signals' vector, and the complex noise vector, respectively. They can be expressed as follows

$$\begin{aligned} \mathbf{D} &= [\mathbf{d}(\theta_1) \dots \mathbf{d}(\theta_m) \dots \mathbf{d}(\theta_M)] , \\ \mathbf{r}(k) &= [r_1(k) \dots r_m(k) \dots r_M(k)]^T , \\ \mathbf{\Omega}(k) &= [\omega_1(k) \dots \omega_n(k) \dots \omega_N(k)]^T , \end{aligned} \tag{6}$$

where $\mathbf{d}(\theta_m) \in \mathbb{C}^{N\times 1}$ is the steering vector of the m-th received signal. For an ULA antenna, it can be expressed as

$$\mathbf{d}(\theta_m) = \begin{bmatrix} e^{i\frac{2\pi}{\lambda}d_1 \sin(\theta_m)} \\ \vdots \\ e^{i\frac{2\pi}{\lambda}d_n \sin(\theta_m)} \\ \vdots \\ e^{i\frac{2\pi}{\lambda}d_N \sin(\theta_m)} \end{bmatrix}. \tag{7}$$

The problem in (5) can be formulated as an optimization problem, the complete unobservable information, i.e. $\mathbf{Dr}(k)$, needs to be estimated from the incomplete observable data, i.e. $\mathbf{x}(k)$. To solve this optimization problem, the SAGE algorithm deploys expectation and maximization steps as follows:

The expectation step

$$\begin{aligned} \mathbf{y}_m(k) &= E\left[\mathbf{y}_m(k)|\mathbf{x}(k), \eta^{\mu}\right] \\ &= \mathbf{d}(\theta_m^{\mu}) r_m^{\mu}(k) + \left(\mathbf{x}(k) - \mathbf{D}^{\mu}\mathbf{r}^{\mu}(k)\right), \end{aligned} \tag{8}$$

where $\mathbf{y}_m(k) \in \mathbb{C}^{N\times 1}$ is the expected m-th received signal's vector, η^{μ} is the estimated parameters matrix and it is given by

$$\begin{aligned} \eta^{\mu} &= \left[\eta_1^{\mu} \dots \eta_m^{\mu} \dots \eta_M^{\mu}\right] \\ \eta_m^{\mu} &= \left[\theta_m^{\mu} \quad r_m^{\mu}(k)\right]^T, \end{aligned} \tag{9}$$

in which η_m^{μ} is the estimated parameters vector of the m-th received signal at the μ-th iteration step, and θ_m^{μ} and $r_m^{\mu}(k)$ are the estimated values of θ_m and $r_m(k)$ at the μ-th iteration step, respectively.

The covariance matrix of the expected m-th signal can be expressed as

$$\mathbf{R}_m = \frac{1}{K}\sum_{k=0}^{K-1} \mathbf{y}_m(k)\mathbf{y}_m^H(k), \tag{10}$$

where $()^H$ is the conjugate transpose notation and K is the total amount of received signals' samples. It is worth mentioning that the term $(\mathbf{x}(k) - \mathbf{D}^{\mu}\mathbf{r}^{\mu}(k))$ in (8) represents the mismatch between the expected values and the observed incomplete data, i.e. the noise in the system.

The maximization step

$$\begin{aligned} \theta_m^{\mu} &= \arg\max_{\theta}\{\mathbf{d}(\theta)^H \mathbf{R}_m \mathbf{d}(\theta)\} \\ r_m^{\mu}(k) &= \frac{1}{N}\mathbf{d}(\theta_m^u)^H \mathbf{y}_m(k), \end{aligned} \tag{11}$$

The E-step in (8) is coupled iteratively with the M-step in (11), as shown in algorithm 1. The algorithm reveals that the parametric search is repeated iteratively until the parametric change satisfies a predefined tolerance ϵ.

D. PARTICLE FILTER IMPLEMENTATION

The particle filter is an important tracking algorithm that can cope with nonlinear and non-Gaussian dynamic motion models[3]. Few attempts have been introduced to deploy the particle filter based on the AoA estimation [35]–[37]. These attempts deal mainly with simulation results and do not involve a specific application. The combination of AoA estimations and the particle filter implementation for a real life IoT application has not yet presented, which constitutes a major contribution of this paper.

[3]For details regarding other tracking filters and the particle filter mathematical background, the reader is referred to [34].

Algorithm 1 SAGE Algorithm

Input: η^0

$\mu \leftarrow 1$
while $\eta^{\mu} - \eta^{\mu-1} > \epsilon$ **do**
  for $m \leftarrow 1$ to M **do**
    E-step:
      calculate $\mathbf{y}_m$, see (8)
      calculate $\mathbf{R}_m$, see (10)
    M-step:
      estimate θ_m^{μ} and $r_m^{\mu}(k)$, see (11)
      $\eta_m^{\mu} = \left[\theta_m^{\mu} \quad r_m^{\mu}(k)\right]^T$
  end for
  $\mu \leftarrow \mu + 1$
end while

Algorithm 2 Particle Filter

Input: Θ^e, P, Z, Z_c, s, $\boldsymbol{\zeta}$, $\boldsymbol{\alpha}$

Algorithm 2: Initialize Z particles.
for $p \leftarrow 1$ to P **do**
  Algorithm 3: predict new particle states.
  Algorithm 4: update particle weights.
  Algorithm 5: resample and state estimate.
end for

Here, we utilized the environmental features (i.e. the angles of the two ends of the pedestrian crossings with respect to the AoA system) in a 1D particle filter. Our implementation has been divided into 5 simple and easy to deploy algorithms. The general implementation of the particle filter is presented in Algorithm 2. The input information to the filter are Θ^e, P, Z, Z_c, s, $\boldsymbol{\zeta}$ and $\boldsymbol{\alpha}$. In which, Θ^e represents the AoA estimations vector and can be expressed as:

$$\Theta^e = [\theta_1^e \dots \theta_p^e \dots \theta_P^e]^T, \tag{12}$$

where P is the total amount of the received signals.[4] θ_p^e is the AoA estimation of the p-th received signal. θ_p^e has been obtained using Algorithm 1.

Z is the total amount of particles and $Z_c(\leq Z)$ is the total amount of particles that share the same statistical behavior. The vectors s, $\boldsymbol{\zeta}$ and $\boldsymbol{\alpha}$ represent the direction of particles' motion, the maximum possible particles' displacement and the initial locations of the particles, respectively. All these

[4]The difference between M and P is that M is the total amount of the received signals from the direct and the reflected paths during a single transmission. The value P, on the other hand, is the total amount of received signals from all the transmissions during the entire operation.

vectors can be presented as follows:

$$\begin{aligned} s &= [s_1 \dots s_i \dots s_{(Z/Z_c)}]^T \\ \boldsymbol{\zeta} &= [\zeta_1 \dots \zeta_i \dots \zeta_{(Z/Z_c)}]^T \\ \boldsymbol{\alpha} &= [\alpha_1 \dots \alpha_i \dots \alpha_{(Z/Z_c)}]^T. \end{aligned} \tag{13}$$

It is worth noting that the AoA estimation is the only measurement that was considered, therefore, all the aforementioned parameters represent the angular behavior of the particles with respect to the AoA estimation system.

Algorithm 3 Initialize Z Particles

1: $z = 1$
2: **for** $i \leftarrow 1$ to Z/Z_c **do**
3: **for** $j \leftarrow 1$ to Z_c **do**
4: $\nu^z \sim s_i \mathcal{R}(\zeta_i)$
5: $\theta^z \sim \mathcal{R}_n(\alpha_i, 1^\circ)$
6: $\chi^z = [\nu^z, \theta^z]$
7: $z = z + 1$
8: **end for**
9: **end for**

The initialization of the particle filter is presented in Algorithm 3. First, the particles will be divided into Z/Z_c subsets of particles that share the same statistical behavior (e.g. if there are two pedestrian crossings and every end of the crossings is represented by 100 particles, then $Z_c = 100$ particles and $Z = 400$ particles). The z-th particle (χ^z) will be represented by two parameters. The first parameter ν^z represents the particle's angular velocity and the second parameter θ^z represents the particle's angle with respect to the AoA estimation system. $\mathcal{R}(\zeta_i)$ is a uniform distribution function that returns a random value between [0 ζ_i], and $\mathcal{R}_n(\alpha_i, 1^\circ)$ is a normal distribution function that returns a random value within the mean value α_i and the standard deviation (std) of 1°. For this application, it is safe to assume that the pedestrians are very close to the edge of the crossing when the pedestrians' traffic light becomes green. Therefore, the small standard deviation (i.e. std $= 1^\circ$) is valid, nonetheless, any other standard deviation value can be applied. Finally, the particles in this model are moving in one dimension, therefore, s_i is assigned $+$ to the right end of the crossing and $-$ to the left end of the crossing.

Algorithm 4 Motion Model

1: **for** $z \leftarrow 1$ to Z **do**
2: $\nu^z \sim \mathcal{R}_n(\nu^z, 1^\circ)$
3: $\theta^z = \theta^z + \nu^z$
4: **end for**

Algorithm 4 represents the motion model of the particles. It can be deducted that the motion model is very simple, therefore, the update of the particles will be done with a minimal computational complexity. Nevertheless, as it will be shown in the results, this motion model was very effective in detecting the direction of the motion and reducing the state estimate error.

Algorithm 5 Update Particle Weights

1: **for** $z \leftarrow 1$ to Z **do**
2: $w^z \sim p\left(\theta^z | \theta_p^e\right)$
3: **end for**
4: **for** $z \leftarrow 1$ to Z **do**
5: $w^z = w^z / \sum_{i=1}^{Z} w^i$
6: **end for**

Algorithm 5 represents the measurement model. In this model, the weight w^z of the z-th particle will be updated with respect to the estimated AoA information. The function $p\left(\theta^z | \theta_p^e\right)$ returns the probability of the particle z that has the correct angle θ^z giving the measured angle θ_p^e. In this paper, we deployed the normal distribution function as the probability function with a standard deviation equals 5°. After computing the weight values for all the particles, the weight of every particle will be divided by the sum of all the weight values to provide a normalized weight vector, as shown in lines 4-6.

Algorithm 6 Cumulative Sum Resample

1: $z = 1$
2: $\beta^1 = w^1$
3: $r = \mathcal{R}(1)$
4: **while** $z <= Z$ **do**
5: **for** $i \leftarrow 2$ to Z **do**
6: $\beta^i = \beta^{i-1} + w^i$
7: **while** $r \leq \beta^i$ **do**
8: $z = z + 1$
9: $\chi^z = \chi^i$
10: $r = \mathcal{R}(1)$
11: **break**
12: **end while**
13: **end for**
14: **end while**
15: **return** $\hat{\theta} = \text{mean}(\theta^{[1,2,\dots,Q]})$

Algorithm 6 represents the resampling algorithm. Several resampling techniques have been introduced in the literature [38]. In this particle filter, we deployed the commutative sum resampling method. The algorithm starts with setting the particle number, setting the first value of the commutative sum vector $\beta^1 = w^1$, and setting a random number between [0 1] to r. The r value will be used as a control value in line 7. The resampling algorithm constitutes three nested loops. The first while loop (lines 4-14) ensures the update of all the particles. The for loop (lines 5-13), on the other hand, calculates the cumulative sum value β^i of the particles' weight. Finally, the second while loop (lines 7-12) compares r with β^i. If the statement $r \leq \beta^i$ is false then the for loop will continue. If the statement $r \leq \beta^i$ is true then the particle number and the state will be updated, and a new random value

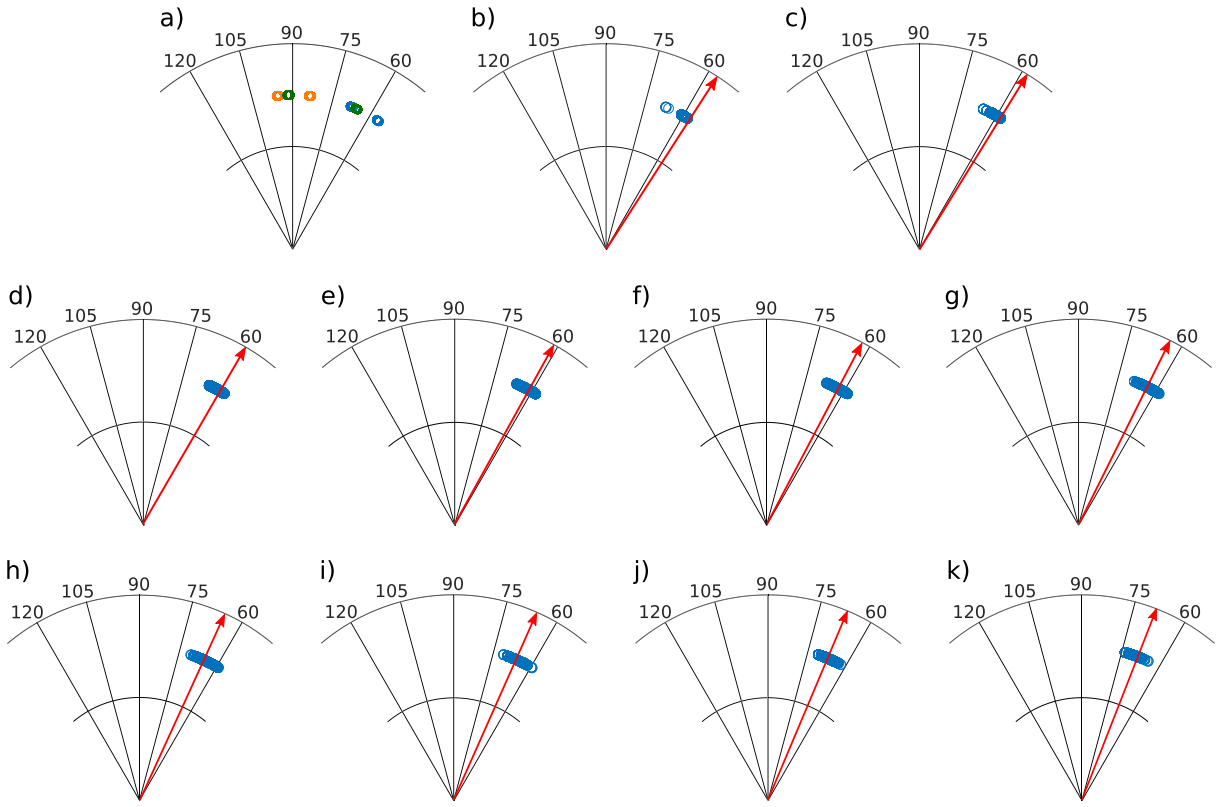

FIGURE 6. The particles development after every AoA estimate of the received signal. In this figure, a single DASH7 signal was transmitted at every white zebra line of the C2 crossing. Figure a) shows the particles distribution before the operation. The red arrows in figures (b-k) represent the actual angular orientation of the white zebra line location with respect to the AoA estimation system. The figure shows, after the first measurement, the particles start to approach the exact location (the red arrow). As the time progresses, the particles keep progressing to provide a mean estimation almost equal to the exact angle.

will be assigned to r. Afterwards, at line 11, the for loop will break to start the resampling process for the next particle. The final step of the resampling process is the calculation of the state estimate. In this paper, the state estimate is taken as the mean of all the particles' angles, as shown in line 15.

IV. SMART CROSSING EXPERIMENTAL RESULTS

We conducted an experiment, in the smart zone of Antwerp city, to validate the proposed localization system. The AoA estimation system was installed on the top of a building that faces an intersection of 5 streets.[5] Every street has its own pedestrian crossing, as shown in Figure 5. The C4 crossing was in the non-line-of-sight (NLoS) region with respect to the AoA estimation system. The C1 crossing, on the other hand, was orthogonal to the estimation axes of the AoA system (i.e. the start and the end of the crossing had the same angle with respect to the AoA estimation system). Therefore, only C2, C3 and C5 crossings have been considered in our analysis. Nonetheless, by optimizing the location of the AoA estimation system, all the crossings can be considered. During the experiment; 10 DASH7 signals, per white zebra line per crossing, were transmitted. A total of 340 DASH7 signals have been transmitted during the experiment.

[5]The total area of the intersection is around 820 m^2. Nonetheless, the utilization of the environmental features constrains the area of interest to the pedestrian crossings only.

The geo-locations of the white zebra lines per crossing have been mapped to the equivalent angles with respect to the AoA estimation system. For the C2 and C3 crossings, the angular difference between two successive white zebra lines was 1° (on average) and for the C5 crossing was 2.16°. According to the described system in Section III, the pedestrian transceiver becomes active when the pedestrian is near one of the two ends of any crossing. The particle filter initialization for both ends of the three crossings is shown in Figure 6 a). The figure shows that the one end of the C5 crossing (the green particles) overlaps with the C2 crossing (the blue particles), and the other end overlaps with the C3 crossing (the orange particles). 500 particles per end per crossing have been used (i.e. $Z_c = 500$), rendering 3000 particles for the complete filter response (i.e. $Z = 3000$). Furthermore, for every crossing, the direction of the particles' motion (i.e. s_i) at the right end of the crossing is opposite to the direction of the particles' motion at the left end of the crossing.

Figure 6 shows the development of the particles after every AoA estimation. In this figure, a single DASH7 signal was transmitted at every white zebra line of the C2 crossing. The red arrows represent the actual angular orientation of the white zebra line location with respect to the AoA estimation system. The C2 crossing has 10 white zebra lines, therefore, 10 DASH7 signals were transmitted. Figures 6 (b-k) show,

FIGURE 7. The direction estimates of three different locations on the C2 crossing. The white arrows represent the directions that are obtained from the particle filter state estimate (i.e. the mean of all the particles' angles as shown in figure 6). The figure demonstrates the feasibility of the proposed solution to provide an accurate estimate of the pedestrian location.

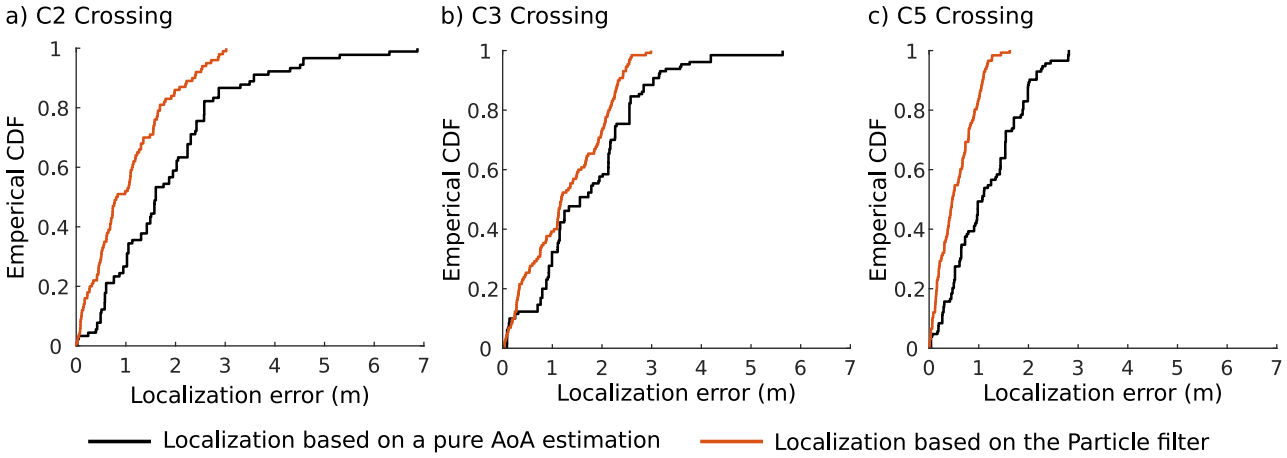

FIGURE 8. The CDF plots of the location estimation error from all the received signals at the C2, C3, and C5 crossings, respectively. The CDF at each figure presents the location estimates based on the pure AoA estimation (using Algorithm 1) and based on the particle filter estimation. The figure reveals that the particle filter has provided a better location estimates than the pure AoA estimation. Furthermore, the locations at the C5 crossing have been estimated with better accuracy than the other two crossings. Nevertheless, the location estimates based on the particle filter are readily very accurate. The median of the estimation error for all the received signals was below 1 meter and the maximum estimation errors for the C2, C3 and C5 crossings were 3, 3.1 and 1.5 meters, respectively.

after the first measurement, all the particles start to approach the exact location (the red arrow). As the time progresses, the particles keep progressing to provide a mean estimation almost equal to the exact angle.

Figure 7 shows the AoA estimates of three different locations on the C2 crossing. The white arrows represent the directions that are obtained from the particle filter state estimate (i.e. the mean of all the particles' angles as shown in Figure 6). The figure demonstrates the feasibility of the proposed solution to provide an accurate estimate of the pedestrian location.

Figure 8 (a, b and c) show the cumulative distribution function (CDF) of the location estimation error from all the received signals at the C2, C3, and C5 crossings, respectively. The CDF at each figure presents the location estimates based on the pure AoA estimation (using Algorithm 1) and based on the particle filter estimation. The figure reveals that the particle filter has provided better location estimates than the pure AoA estimation. Furthermore, the locations at the C5 crossing have been estimated with a better accuracy than the other two crossings. This can be attributed to the fact that the position of the C5 crossing is the closest to the AoA unit compared with the other two crossings. Therefore, the LoS condition is almost certain for the C5 crossing, consequentially, the exact location can be retrieved. Nevertheless, the location estimates based on the particle filter are readily very accurate. The median of the estimation error for all the received signals was below 1 meter and the maximum estimation errors for the C2, C3 and C5 crossings were 3, 3.1 and 1.5 meters, respectively.

The AoA estimation is expected to be improved with enlarging the array antenna aperture and with optimizing the AoA estimation system's location.

V. CONCLUSION

In this paper, we presented a simple yet efficient localization system that is suitable for locating people over a pedestrian crossing. By adopting the proposed localization system, the people flow over the pedestrian crossing can be observed. Consequently, a safe and an efficient traffic flow in the smart city can be achieved. The proposed system utilizes IoT transceivers carried by the pedestrians (or embedded in the pedestrians' smart devices). These transceivers can be activated to transmit a signal every few seconds when the pedestrian passes over a pedestrian crossing. These periodic signals will be received by a single AoA estimation system

to estimate the direction of the pedestrian. Furthermore, the pedestrian direction and the environmental features of the pedestrian crossings are utilized in a 1D particle filter to estimate accurately the pedestrian location.

The proposed system consists of two main modes: the waiting and the localization modes. The IoT transceiver stays in the waiting mode until it receives an enabling signal, afterwards, the system switches to the localization mode. The main focus of this paper is to investigate the localization capability of the proposed system. Therefore, the waiting mode has neither implemented nor investigated. The investigation of the waiting mode will constitute the focus of the future work.

The localization mode has been experimentally validated in the smart zone of Antwerp city. The AoA estimation system was installed on the top of a building that faces an intersection of 5 streets. The experimental results reveal that the proposed localization system can provide an accurate, cost effective and reliable localization solution to this specific problem without violating the pedestrian privacy.

ACKNOWLEDGMENT

The authors would like to thank the city of Antwerp and the institute of tropical medicine for allowing us to use their public space and buildings for our investigations.

REFERENCES

[1] *LoRa Alliance*. Accessed: Jul. 30, 2020. [Online]. Available: https://lora-alliance.org/
[2] *Sigfox*. Accessed: Jul. 30, 2020. [Online]. Available: https://www.sigfox.com/en
[3] *Standardization of NB-IOT*. Accessed: Jul. 30, 2020. [Online]. Available: https://www.3gpp.org/news-events/1785-nb_iot_complete
[4] *DASH7 Alliance*. Accessed: Jul. 30, 2020. [Online]. Available: https://dash7-alliance.org
[5] A. Zanella, N. Bui, A. Castellani, L. Vangelista, and M. Zorzi, "Internet of Things for smart cities," *IEEE Internet Things J.*, vol. 1, no. 1, pp. 22–32, Feb. 2014.
[6] *Smart Zone*. Accessed: Jul. 30, 2020. [Online]. Available: https://antwerpsmartzone.be/en
[7] G. Pau, T. Campisi, A. Canale, A. Severino, M. Collotta, and G. Tesoriere, "Smart pedestrian crossing management at traffic light junctions through a fuzzy-based approach," *Future Internet*, vol. 10, no. 2, p. 15, Feb. 2018.
[8] Z. Zhang, L. Jia, and Y. Qin, "Level-of-service based hierarchical feedback control method of network-wide pedestrian flow," *Math. Problems Eng.*, vol. 2016, pp. 1–14, Jan. 2016.
[9] C.-J. Zheng, R. He, X. Wan, and C. Wang, "The study on in-city capacity affected by pedestrian crossing," *Math. Problems Eng.*, vol. 2016, pp. 1–8, Jan. 2016.
[10] *SMART Pedestrian Crossing*. Accessed: Jul. 30, 2020. [Online]. Available: http://countmein.eu/smartchange/smart-pedestrian-crossing
[11] *Intelligent Pedestrian Traffic Lights: New System by TU Graz Automatically Recognises Pedestrians' Intent to Cross the Road*. Accessed: Jul. 30, 2020. [Online]. Available: https://www.tugraz.at/en/tu-graz/services/news-stories/media-service/si%ngleview/article/denkende-fussgaengerampeln-neues-system-der-tu-graz-erkennt%-kreuzungswunsch-automatisch0
[12] *Pedestrian Radar*. Accessed: Jul. 30, 2020. [Online]. Available: https://www.agd-systems.com/agdproduct/326-pedestrian-radar/
[13] A. Ghosh, A. Maeder, M. Baker, and D. Chandramouli, "5G evolution: A view on 5G cellular technology beyond 3GPP release 15," *IEEE Access*, vol. 7, pp. 127639–127651, 2019.
[14] N. Bnilam, E. Tanghe, J. Steckel, W. Joseph, and M. Weyn, "ANGLE: ANGular location estimation algorithms," *IEEE Access*, vol. 8, pp. 14620–14629, 2020.
[15] M. Aernouts, N. BniLam, R. Berkvens, and M. Weyn, "Simulating a combination of TDoA and AoA localization for LoRaWAN," in *Proc. Int. Conf. P2P, Parallel, Grid, Cloud Internet Comput.* Antwerp, Belgium: Springer, 2019, pp. 756–765.
[16] T. Janssen, M. Aernouts, R. Berkvens, and M. Weyn, "Outdoor fingerprinting localization using sigfox," in *Proc. Int. Conf. Indoor Positioning Indoor Navigat. (IPIN)*, Sep. 2018, pp. 1–6.
[17] N. BniLam, G. Ergeerts, D. Subotic, J. Steckel, and M. Weyn, "Adaptive probabilistic model using angle of arrival estimation for IoT indoor localization," in *Proc. Int. Conf. Indoor Positioning Indoor Navigat. (IPIN)*, Sep. 2017, pp. 1–7.
[18] W. Gong and J. Liu, "RoArray: Towards more robust indoor localization using sparse recovery with commodity WiFi," *IEEE Trans. Mobile Comput.*, vol. 18, no. 6, pp. 1380–1392, Jun. 2019.
[19] E. Y. Menta, N. Malm, R. Jantti, K. Ruttik, M. Costa, and K. Leppanen, "On the performance of AoA—Based localization in 5G ultra–dense networks," *IEEE Access*, vol. 7, pp. 33870–33880, 2019.
[20] Z. Yang and W. Gong, "Decimeter-level WiFi tracking in real-time," in *Proc. IEEE/ACM 28th Int. Symp. Qual. Service (IWQoS)*, Jun. 2020, pp. 1–10.
[21] S. Tomic, M. Beko, R. Dinis, and L. Bernardo, "On target localization using combined RSS and AoA measurements," *Sensors*, vol. 18, no. 4, p. 1266, Apr. 2018.
[22] *EZR32LG330 Data Sheet*. Accessed: Jul. 30, 2020. [Online]. Available: https://www.silabs.com/documents/public/data-sheets/EZR32LG330_DataShee%t.pdf
[23] M. Weyn, G. Ergeerts, R. Berkvens, B. Wojciechowski, and Y. Tabakov, "DASH7 alliance protocol 1.0: Low-power, mid-range sensor and actuator communication," in *Proc. IEEE Conf. Standards Commun. Netw. (CSCN)*, Oct. 2015, pp. 54–59.
[24] J. Steckel, D. Laurijssen, A. Schenck, N. BniLam, and M. Weyn, "Low-cost hardware platform for angle of arrival estimation using compressive sensing," in *Proc. 12th Eur. Conf. Antennas Propag. (EuCAP)*, Apr. 2018, pp. 1–4.
[25] N. BniLam, J. Steckel, and M. Weyn, "Synchronization of multiple independent sub-array antennas for IoT applications," in *Proc. 12th Eur. Conf. Antennas Propag. (EuCAP)*, Apr. 2018, pp. 1–5.
[26] N. BniLam, A. Aerts, D. Joosens, J. Steckel, and M. Weyn, "RSS-based AoA estimation system for IoT applications using rotman lens," in *Proc. 14th Eur. Conf. Antennas Propag. (EuCAP)*, Mar. 2020, pp. 1–5.
[27] K.-J. Baik, S. Lee, and B.-J. Jang, "Hybrid RSSI-AoA positioning system with single time-modulated array receiver for LoRa IoT," in *Proc. 48th Eur. Microw. Conf. (EuMC)*, Sep. 2018, pp. 1133–1136.
[28] G. Avitabile, A. Florio, and G. Coviello, "Angle of arrival estimation through a full-hardware approach for adaptive beamforming," *IEEE Trans. Circuits Syst. II, Exp. Briefs*, vol. 67, no. 12, pp. 3033–3037, Dec. 2020.
[29] N. BniLam, D. Joosens, J. Steckel, and M. Weyn, "Low cost AoA unit for IoT applications," in *Proc. 13th Eur. Conf. Antennas Propag. (EuCAP)*, Mar. 2019, pp. 1–5.
[30] *RTL-SDR*. Accessed: Jul. 30, 2020. [Online]. Available: https://www.rtl-sdr.com/
[31] N. BniLam, D. Joosens, M. Aernouts, J. Steckel, and M. Weyn, "LoRay: AoA estimation system for long range communication network," *IEEE Trans. Wireless Commun.*, early access, Nov. 24, 2020, doi: 10.1109/TWC.2020.3038565.
[32] B. H. Fleury, M. Tschudin, R. Heddergott, D. Dahlhaus, and K. Ingeman Pedersen, "Channel parameter estimation in mobile radio environments using the SAGE algorithm," *IEEE J. Sel. Areas Commun.*, vol. 17, no. 3, pp. 434–450, Mar. 1999.
[33] P. J. Chung and J. F. Böhme, "DOA estimation using fast EM and SAGE algorithms," *Signal Process.*, vol. 82, no. 11, pp. 1753–1762, Nov. 2002.
[34] M. S. Arulampalam, S. Maskell, N. Gordon, and T. Clapp, "A tutorial on particle filters for online nonlinear/non-Gaussian Bayesian tracking," *IEEE Trans. Signal Process.*, vol. 50, no. 2, pp. 174–188, Aug. 2002.
[35] W. Ng, J.-R. Larocque, and J. P. Reilly, "On the implementation of particle filters for DOA tracking," in *Proc. IEEE Int. Conf. Acoust., Speech, Signal Process.*, May 2001, pp. 2821–2824.
[36] A. Papaiz and A. M. Tonello, "Particle filtering with weight reshaping for opportunistic angle of arrival estimation in a vehicular scenario," in *Proc. IEEE 5th Int. Conf. Consum. Electron. Berlin (ICCE-Berlin)*, Sep. 2015, pp. 145–149.
[37] H. Seo, H. Kim, J. Kang, I. Jeong, W. Ahn, and S. Kim, "3D moving target tracking with measurement fusion of TDoA/FDoA/AoA," *ICT Exp.*, vol. 5, no. 2, pp. 115–119, Jun. 2019.
[38] T. Li, M. Bolic, and P. M. Djuric, "Resampling methods for particle filtering: Classification, implementation, and strategies," *IEEE Signal Process. Mag.*, vol. 32, no. 3, pp. 70–86, May 2015.